Low-temperature magnetic and transport properties of layered Sr_xCoO_2

Y. Q. Guo, J. L. Luo,* G. T. Liu, H. X. Yang, J. Q. Li, N. L. Wang, and D. Jin
Beijing National Laboratory for Condensed Matter Physics, Institute of Physics, Chinese Academy of Sciences, P.O. Box 603, Beijing 100080, People's Republic of China

T. Xiang
Institute of Theoretical Physics, Chinese Academy of Sciences, P.O. Box 2735, Beijing 100080, People's Republic of China

(Received 7 April 2006; revised manuscript received 29 July 2006; published 30 October 2006)

A series of polycrystalline samples of Sr_xCoO_2 ($0.15 \leq x \leq 0.40$) have been prepared by a low-temperature ion exchange technique. These Sr_xCoO_2 samples are isomorphic to Na_xCoO_2 with the hexagonal structure, but behave differently from Na_xCoO_2 with the change of cation concentration. For all the samples, the magnetic susceptibility decreases with increasing temperature and shows a Curie-Weiss behavior at high temperatures. The low-temperature magnetic susceptibility can be changed considerably by an applied field. The specific-heat coefficient $\gamma = C/T$ of Sr_xCoO_2 as a function of T^2 turns downwards at low temperatures. This is different from the upturn behavior of low-temperature γ in Na_xCoO_2. The resistivity of Sr_xCoO_2 changes significantly with the strontium content x. An insulating to metallic crossover or transition is observed with increasing x.

DOI: 10.1103/PhysRevB.74.155129 PACS number(s): 75.20.Hr, 71.27.+a, 72.80.Ga, 82.30.Hk

I. INTRODUCTION

The recent discovery of superconductivity at ~5 K in $Na_{0.35}CoO_2 \cdot 1.3H_2O$ has attracted much attention in the study of layered compounds Na_xCoO_2.[1,2] The structure of Na_xCoO_2 consists of alternate stacking of Na and CoO_2 layers along the c axis and Co ions in each CoO_2 sheet form triangular lattices. A striking feature of this system is that Na_xCoO_2 possesses rich physical properties varying sensitively with the Na concentration.[1,3–8] Transport measurements revealed that Na_xCoO_2 exhibits a metallic behavior in the whole Na compositions except for $x=0.5$, which becomes a charge-ordered insulator at 53 K. As x varying from $x \sim 0.7$ to $x \sim 0.3$, the susceptibility (χ) of Na_xCoO_2 crosses over from a Curie-Weiss behavior for $x > 0.5$ to a Pauli paramagnetic behavior for $x < 0.5$. The χ of $Na_{0.5}CoO_2$ decreases with decreasing temperature and exhibits three phase transitions at 87, 53, and 25 K, respectively. For $x \geq 0.75$, an antiferromagnetic transition at about 20 K has been studied by thermodynamic, transport, and muon spin rotation (μSR) measurements.[6,8–10]

To gain more insight into the Na_xCoO_2 system, the search and investigation of other triangular lattice systems isostructural with Na_xCoO_2 are of great interest. It is well known that physical properties of high-T_c cuprates are mainly determined by the physics of Cu-O planes, and different high-T_c compounds possess similar physical properties and can be described by a generic phase diagram. It is interesting to see if other cobaltites with triangular Co lattices possess similar physical properties as Na_xCoO_2.

Substitution of Na ions with divalent ions has attracted considerable attention.[11–18] Ryuji Ishikawa *et al.*[16] first synthesized γ-$Sr_{0.35}CoO_2$ by a low-temperature ion exchange technique from a γ-$Na_{0.7}CoO_2$ precursor and studied its transport and thermoelectric properties. $Sr_{0.35}CoO_2$ possesses a similar crystal structure as Na_xCoO_2. Its Seebeck coefficient is comparable to that of γ-$Na_{0.7}CoO_2$, and the resistivity shows a metallic behavior, in agreement with the band-structure calculation.[17] Structural analysis suggested that Sr_xCoO_2 has hexagonal symmetry, similar to γ-Na_xCoO_2($P6_3/mmc$). Two superstructures arising respectively from the ordering of intercalated Sr and a periodic structural distortion were observed in $Sr_{0.35}CoO_2$.[18]

In this paper, we report the synthesis of polycrystalline Sr_xCoO_2 ($0.15 \leq x \leq 0.40$) and their low-temperature magnetic susceptibility, specific-heat, and electrical resistivity measurements. Physical properties of Sr_xCoO_2 are then compared with Na_xCoO_2 to see whether the T-x phase diagram of Na_xCoO_2 is of generic feature.

II. SAMPLE PREPARATION AND CHARACTERIZATION

Polycrystalline samples of Sr_xCoO_2 ($0.15 \leq x \leq 0.40$) were synthesized by a low-temperature ion exchange technique from Na_xCoO_2 ($0.3 \leq x \leq 0.80$) precursors. The ion exchange process was similar to those reported by Cushing and Wiley.[15] The polycrystalline precursors, Na_xCoO_2 ($x \geq 0.7$), were prepared from Na_2CO_3 and Co_3O_4 by a conventional solid-state reaction. The well-mixed powders were heated at 750 °C overnight, and then reground and heated at 850 °C for a day. The Na_xCoO_2 samples with lower sodium concentrations were prepared by chemically deintercalating sodium from $Na_{0.7}CoO_2$ using bromine or iodine as an oxidizing agent, similar to that described in Ref. 4. The precusors were ground together with 10% mol excess anhydrous $Sr(NO_3)_2$ powder and heated in air at 310 °C for two days. The substitution of Na ions with Sr ions occurred during the low-temperature ion exchange process. The soluble $NaNO_3$ and excess $Sr(NO_3)_2$ were removed by repeatedly grinding the products under distilled water. After washing, the products were dried at 120 °C in air for more than 12 h, and then stored in a dry desiccator. The crystal structures and the chemical compositions of these samples were determined by powder x-ray diffraction (XRD) analysis and induction-coupled plasma measurements (ICP), respectively.

 ©2006 The American Physical Society

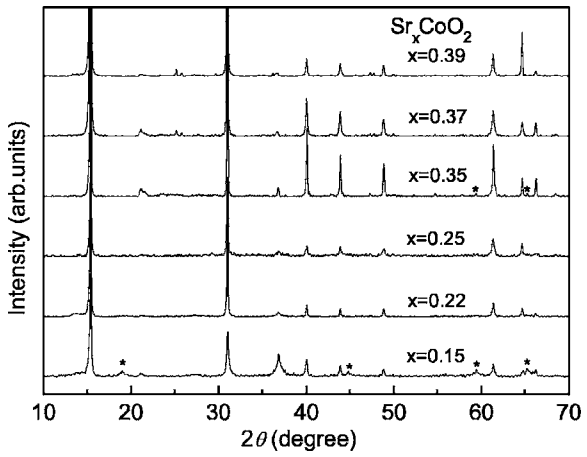

FIG. 1. XRD patterns for polycrystalline Sr_xCoO_2 with $x=0.39$, 0.37, 0.35, 0.25, 0.22, and 0.15, respectively. The asterisks denote the peaks of Co_3O_4.

Figure 1 shows the XRD patterns of Sr_xCoO_2. It indicates that all these samples are isomorphic to γ-Na_xCoO_2 and the diffraction peaks can be indexed on a hexagonal unit cell with the space group of $P6_3/mmc$. This agrees with the previous structural analysis of cobalt oxides γ-A_xCoO_2 (A=Na, Ca, Sr, and Ba).[12,15,16,18] Careful analysis further indicates that there is no impurity in our Sr_xCoO_2 samples with $x>0.35$. However, for the $x=0.35$ and 0.15 samples, some weak diffraction peaks from a tiny trace of Co_3O_4 impurities are observed, marked by asterisks in the figure. There may also exist few Co_3O_4 in other Sr_xCoO_2 samples with $x<0.35$, although there is no trace of the impurities in the XRD patterns.

Figure 2 compares the XRD patterns of Sr_xCoO_2 ($x=0.35$ and 0.37) with their precursors. The patterns show that $Sr_{0.37}CoO_2$ is indeed isostructural with γ-$Na_{0.75}CoO_2$ and no Co_3O_4 peaks are observed in both cases. Some weak Co_3O_4 diffraction peaks are observed in the patterns of $Sr_{0.35}CoO_2$ and its precursor. Compared to their precursors, the peaks of Sr_xCoO_2 shift toward lower 2θ range with the increase of ionic radii from Na to Sr. The lattice parameters change from $a=2.835$ Å, $c=10.879$ Å for $Na_{0.75}CoO_2$ to $a=2.822$ Å, $c=11.523$ Å for $Sr_{0.37}CoO_2$. It is found that there is much less change in lattice parameter a than that in c, implying the substitution occurs in the Na^+ planes and only varies the interlayer spacing. The increasing of c-axis parameter c after the substitution is due to the fact that the radius of Sr^{2+} is larger than Na^+.

The actual atom ratio of these samples is determined by ICP measurements. In Fig. 3, the Sr content of Sr_xCoO_2 is plotted against the Na content of the corresponding precursors. The Sr^{2+} content of each Sr_xCoO_2 sample is equal to one-half the Na^+ content of its precursor and no residual sodium is detected.

The lattice parameters were determined by least-square calculations of 2θ values calibrated using Si as an internal standard. Figure 4 compares the c-axis lattice parameters of Sr_xCoO_2 with their precursors. Different to its precursor, we find that c is almost unchanged with the Sr content in Sr_xCoO_2. This suggests that the greater electrostatic interaction between Sr^{2+} and O^{2-} is enough to overcome the repulsion among the negatively charged layers. A similar relationship between the $[CoO_2]_n$ layer-spacing and the composition in Ca_xCoO_2 was observed.[15,19]

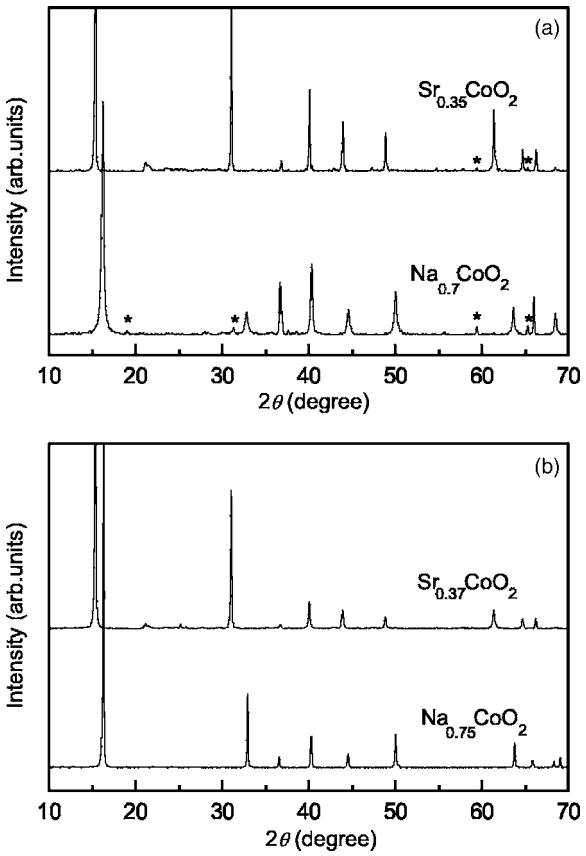

FIG. 2. Comparison of the XRD patterns of Sr_xCoO_2 ($x=0.35$ and 0.37) with their precursors. The asterisks denote the peaks of Co_3O_4.

Previously, we have reported a thermogravimetric analysis (TGA) on $Sr_{0.35}CoO_2$ in the oxygen atmosphere.[18] In order to understand the thermal stability of the Sr-poor samples, we performed a thermogravimetric analysis on the $x=0.15$ sample in air with a sweep rate of 10°C min^{-1}. Figure 5 shows the TGA curve for $Sr_{0.15}CoO_2$ from room tem-

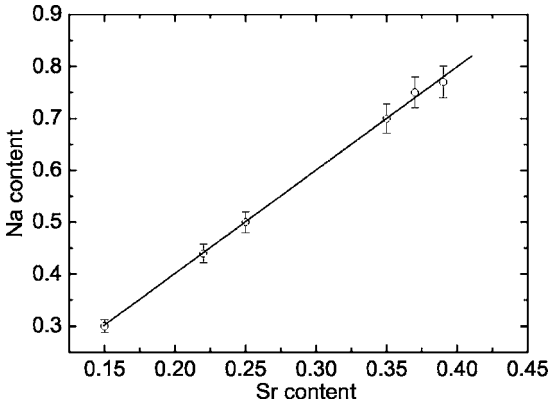

FIG. 3. The Sr content in Sr_xCoO_2 vs the Na content in the corresponding precursor Na_xCoO_2.

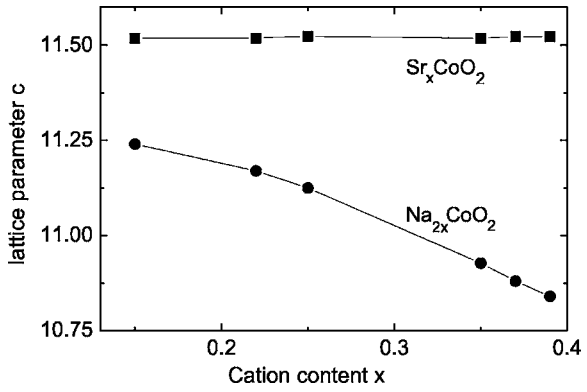

FIG. 4. Variation of the c-axis lattice parameter c as a function of cation content x.

perature to 1000°C. The curve shows that the weight loss below 420°C is about 3%, corresponding to water content of about 0.18 per formula, and the decomposition begins near 530°C. Furthermore, no expansion of the lattice parameter c is observed in the XRD measurements on Sr-poor samples. These results suggest that there is no interlayer crystal water, and the small weight loss is mostly due to the loss of the absorbed intergrain water. However, we cannot rule out the possibility of a very small quantity of $(H_3O)^+$ ions inserting into the Sr planes as in $Na_x(H_3O)_zCoO_2 \cdot nH_2O$.[20] On the contrary, Na-poor samples can readily absorb water to form a series of hydrated phases, and a substantial weight loss is observed on heating due to the dehydration reaction.[21] Moreover, for the Na-poor samples, the insertion of interlayer crystal water is accompanied by a large expansion of the lattice parameter c.

In order to study the effect of air exposure on the Sr-poor samples, we compare the XRD patterns of as-prepared powders and the powders' exposure to air after 3 days. In contrast to the structure transformation of CoO_2 on exposure to air,[22] the crystal structures as revealed by XRD remain almost unchanged. Thus the samples are stable against air exposure. This is similar to Ca_xCoO_2, whose crystal structure is also found to be stable against air or moisture exposure.[15] Thus M_xCoO_2 (M=Sr,Ca) are much more stable than their analogous Na_xCoO_2 materials.[18,19,23]

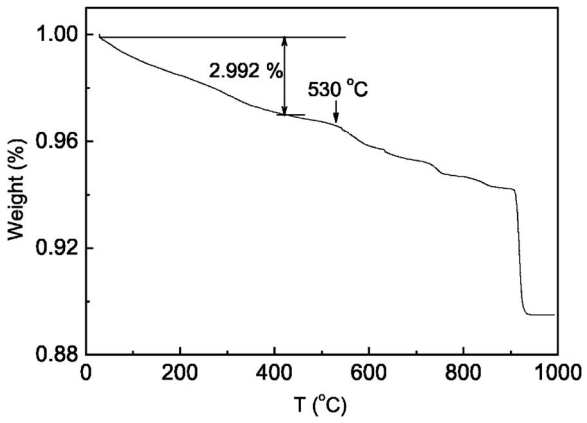

FIG. 5. TGA curve for $Sr_{0.15}CoO_2$ heated in air from room temperature to 1000°C with a heating rate of 10°C min^{-1}.

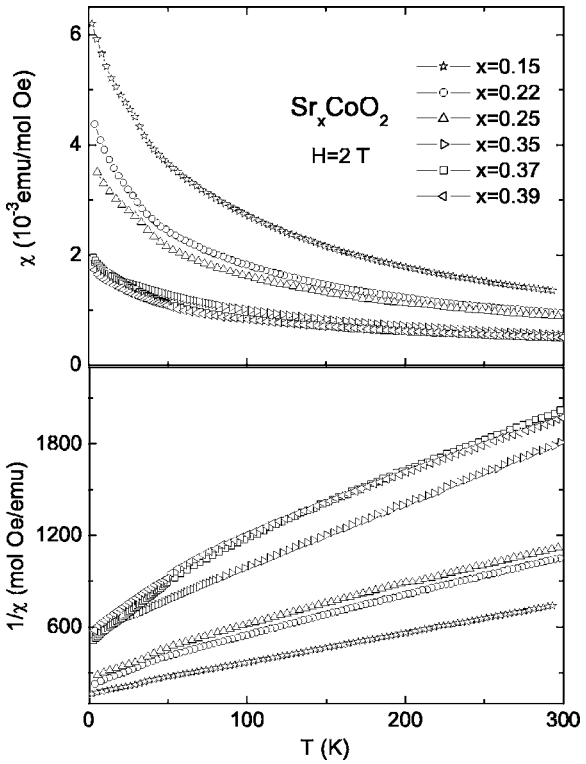

FIG. 6. Temperature dependence of the magnetic susceptibility and inverse susceptibility of Sr_xCoO_2 (H=2 T).

The magnetic susceptibility, specific heat, and resistivity measurements were performed with a Quantum Design physical properties measurement system (PPMS). The specific heat was measured using the relaxation method and the field dependence of the thermometer and addenda was carefully calibrated before the specific-heat measurements. The electrical resistivity was measured using a four-probe method. For electrical resistivity measurements, the pellets were sintered at 400°C for 24 h under flowing O_2 gas. The XRD patterns of the sintered pellets showed no difference to those of the initial powder samples, demonstrating the stability of the samples during the process of sintering at 400°C. Thermogravimetric analysis of the Sr_xCoO_2 samples indicated an onset of decomposition above 500°C, also confirming the thermal stability of the samples after sintering at 400°C.

III. RESULTS AND DISCUSSION

A. Magnetic susceptibility

Figure 6 shows the temperature dependence of the dc magnetic susceptibility χ and the inverse susceptibility of polycrystalline Sr_xCoO_2 in an applied field of 2 T. The magnetic susceptibility increases with decreasing temperature and shows a Curie-Weiss-like behavior at high temperatures for all the samples, though a deviation is noticed at low temperatures, indicating an increase of the magnetic interaction. The value of χ of Sr_xCoO_2 decreases with increasing x, implying a decrease of the magnetic moments. At about 30 K, a small kink appears for $Sr_{0.15}CoO_2$, $Sr_{0.25}CoO_2$, and

TABLE I. Curie-weiss fitting parameters for Sr_xCoO_2.

x	χ_0 ($\times 10^{-3}$) [emu/(mol Oe)]	C ($\times 10^{-3}$) [emu K/(mol Oe)]	Θ (K)	M_{eff} μ_B/Co
0.15	0.04	499.29	−86.96	1.997
0.22	0.12	318.84	−87.81	1.597
0.25	0.20	280.67	−80.71	1.498
0.35	0.04	217.92	−125.03	1.320
0.37	0.18	120.55	−81.04	0.982
0.39	0.23	109.99	−85.30	0.938

$Sr_{0.35}CoO_2$. This is probably due to the antiferromagnetic ordering transition of Co_3O_4. Above 50 K, the data in Fig. 6 are fitted with the following formula:

$$\chi(T) = \chi_0 + C/(T-\theta),$$

where χ_0 is the contribution of temperature-independent magnetic susceptibility, $C/(T-\theta)$ is the Curie-Weiss term due to local Co magnetic moments, C is the Curie constant, and θ is the Weiss temperature. The fitting parameters are shown in Table I. The effective moments M_{eff} of Co ions are determined from the fitting parameters C.

The average formal valence of Co is fractional in Sr_xCoO_2. This is attributed to the coexistence of Co^{3+} and Co^{4+} as in Na_xCoO_2.[24] In Sr_xCoO_2, the occupancy of Co^{4+} spins on the two-dimensional triangular lattices decreases with increasing x: a fraction $2x$ of the Co ions are in the Co^{3+} state, while the rest $(1-2x)$ are in the Co^{4+} state. The Curie-Weiss behavior in the magnetic susceptibility is believed to be induced by the magnetic Co^{4+} ions. The effective moment M_{eff} of Sr_xCoO_2 decreases with increasing x, due to the decreasing concentration of Co^{4+} ions. The Weiss temperature of Sr_xCoO_2 is negative. This suggests that the exchange coupling between local moments is antiferromagnetic.

The variance of temperature dependence of the magnetic susceptibility of Sr_xCoO_2 with the cation concentration differs from that of Na_xCoO_2. The susceptibility of Na_xCoO_2 changes from a Curie-Weiss-like behavior for $x>0.5$ to a relatively T-independent Pauli paramagnetic behavior for $x<0.5$.[1] The Curie-Weiss behavior of Sr_xCoO_2 at low Sr content contrasts strongly with the relatively T-independent Pauli paramagnetic behavior of Na_xCoO_2 for $x<0.5$.

To see more clearly the low-temperature behavior of Sr_xCoO_2, we measured the field dependence of the susceptibility. Figure 7 shows the dc susceptibility of $Sr_{0.37}CoO_2$ in various applied fields up to 12 T. The susceptibility decreases with increasing fields at low temperatures. Similar field dependence is also observed in other Sr_xCoO_2 samples. The susceptibility of Co_3O_4 increases with increasing fields at low temperatures and exhibits a peak around 30 K. This peak structure is not observed in $Sr_{0.37}CoO_2$ around 30 K. This indicates that Co_3O_4 is indeed absent in this sample, consistent with the x-ray-diffraction data. The low-temperature susceptibility of Sr_xCoO_2 in an applied field behaves similarly as in Na_xCoO_2. The decrease of the susceptibility with the field might be also due to an antiferromagnetic interlayer coupling like in Na_xCoO_2.[8,25–29]

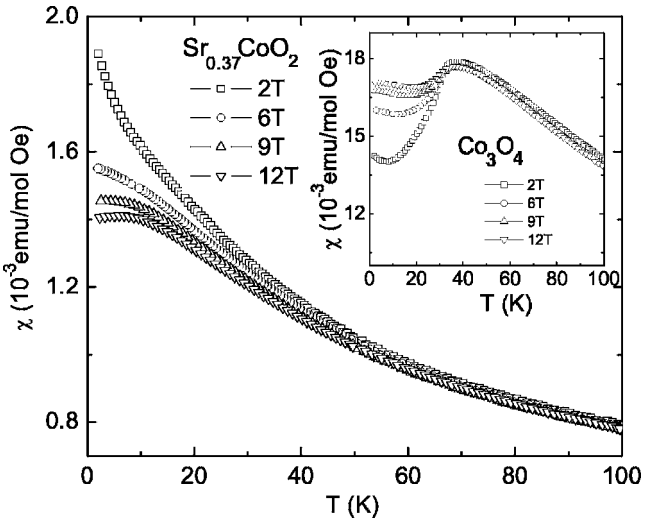

FIG. 7. Temperature dependence of the magnetic susceptibility $\chi(T)$ for $Sr_{0.37}CoO_2$ in various applied fields. The inset shows the magnetic susceptibility for Co_3O_4 in different fields.

In low fields, the paramagnetism arising from paramagnetic impurities or defects prevails over the antiferromagnetic coupling at low temperatures. However, the moments of paramagnetic impurities or defects may become saturated with increasing field. So the susceptibility is suppressed by the increasing fields and shows a shallow and broad peak at low temperatures. The presence of this broad peak at low temperatures provides evidence for antiferromagnetic coupling in the ground state of Sr_xCoO_2. This is consistent with the negative Weiss temperature for Sr_xCoO_2.

B. Specific heat

Figure 8 shows the temperature dependence of the specific heat between 2 and 30 K for Sr_xCoO_2 with $x=0.22$, 0.25, and 0.35. The specific heat decreases monotonically with decreasing temperature for these three samples. If the specific heat is contributed only by the thermal excitations of electrons (a linear T term) and phonons (a T^3 term), the C/T-T^2 curve would exhibit a linear behavior at low T. However, the C/T-T^2 curve of Sr_xCoO_2, as shown in Fig. 8(b), bends downwards at low temperatures. This downturn feature of the specific heat is not observed in Na_xCoO_2 compounds. It suggests that the electron excitations are considerably suppressed at very low temperatures.

From Fig. 8(b), the electronic specific-heat coefficient γ, determined from the C/T data from 4 to 10 K, is found to be 28.71, 28.02, and 23.73 mJ/mol K^2 for $Sr_{0.35}CoO_2$, $Sr_{0.25}CoO_2$, and $Sr_{0.22}CoO_2$, respectively. The contribution from Co_3O_4 impurities, as can be seen from the inset of Fig. 9, is very small below 10 K, and can be ignored in this analysis. These γ values are close to the corresponding values 25–30 mJ/mol K^2 for Na_xCoO_2 ($x=0.7$–0.75).[6,30] The large γ could reflect a large density of states at the Fermi level.

Figure 9 compares the temperature dependence of the specific heat for $Sr_{0.22}CoO_2$ and $Sr_{0.37}CoO_2$. A small peak at about 30 K is observed in the C-T curve for $Sr_{0.22}CoO_2$.

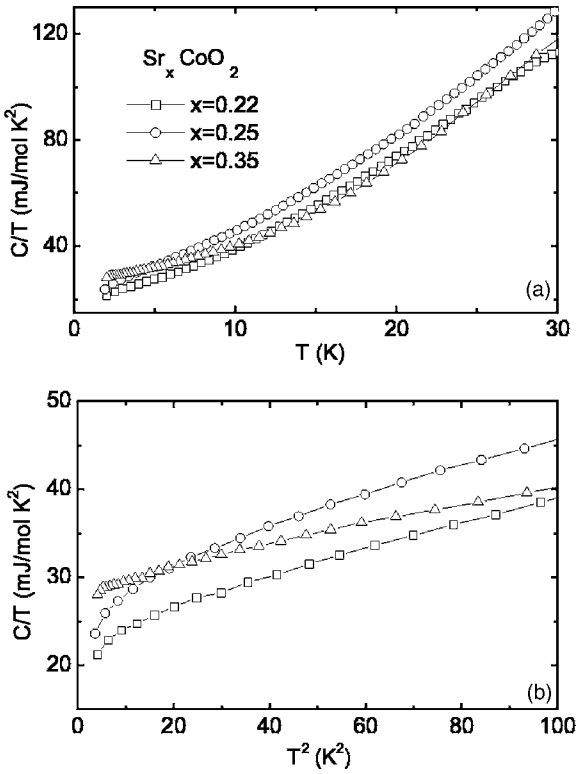

FIG. 8. (a) The C/T vs T and (b) C/T vs T^2 for Sr_xCoO_2 in zero field.

This, as suggested by the inset of Fig. 9, is due to the contribution of Co_3O_4 impurities in this sample, although the trace of Co_3O_4 was not found in the XRD pattern. The amount of Co_3O_4, deduced from the relative height of the peak for $Sr_{0.22}CoO_2$ to that of pure Co_3O_4, is about 2%. However, the specific-heat measurement for the $Sr_{0.37}CoO_2$ sample shows no sign of Co_3O_4 impurities, consistent with our x-ray-diffraction pattern and magnetic susceptibility data.

Compared to Sr_xCoO_2, the C/T-T^2 curve of Na_xCoO_2 shows a different behavior at low temperatures. The curve

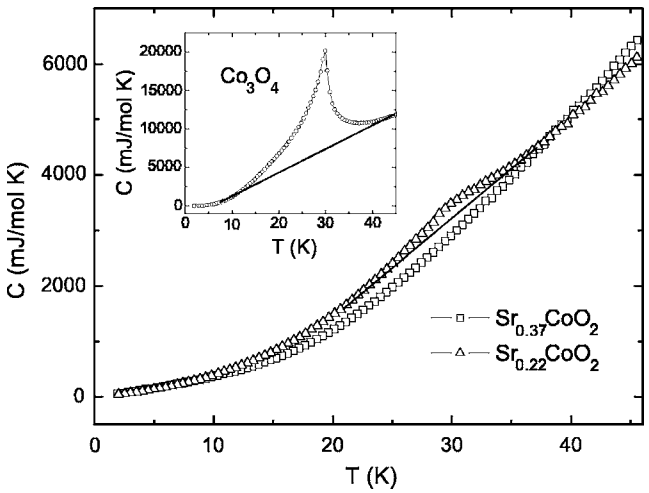

FIG. 9. Temperature dependence of the specific heat C for $Sr_{0.22}CoO_2$ and $Sr_{0.37}CoO_2$ in zero field. The inset shows the C-T curve for Co_3O_4 in zero field.

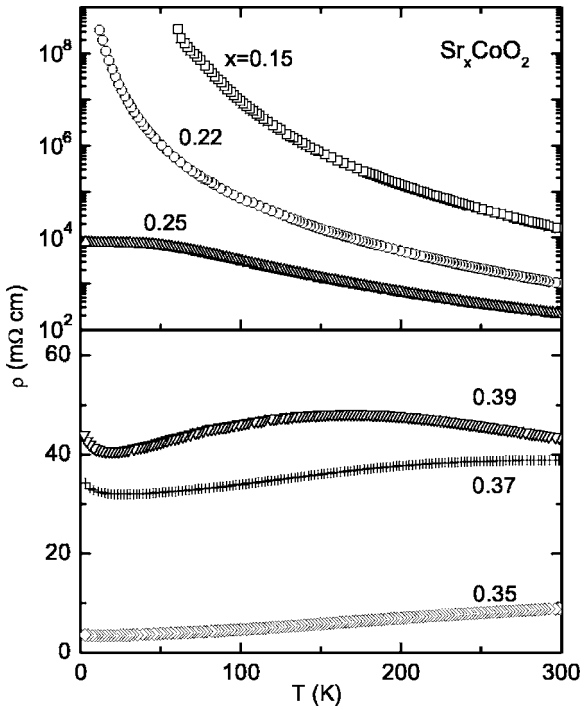

FIG. 10. Resistivity as a function of temperature for Sr_xCoO_2.

deviates upwards from linearity, indicating an additional contribution takes place at low temperatures, which was attributed to the Schottky effect.[12,31]

C. Resistivity

Figure 10 shows the electrical resistivity of the polycrystalline Sr_xCoO_2 as a function of temperature. $\rho(T)$ is sensitive to the strontium content. With increasing x, a crossover from insulating to metallic behaviors is observed. The room-temperature resistivity is 15.6 Ω cm and 987 mΩ cm for the two insulating samples, $x=0.15$ and 0.22, respectively. These values of resistivity are larger than the metallic limit for polycrystalline samples. These two samples pelletized at high pressure of 5 GPa also show insulating behaviors. For $Sr_{0.25}CoO_2$, $\rho(T)$ increases with decreasing temperature down to about 50 K and then shows a plateau at low temperatures.

$Sr_{0.35}CoO_2$ exhibits a metallic resistivity behavior, in agreement with the band-structure calculation.[17] The resistivity of $Sr_{0.35}CoO_2$ is 8.83 mΩ cm at 300 K. This agrees with the data published by Ishikawa *et al.*[16] The resistivity of $Sr_{0.35}CoO_2$ is larger than that of γ-$Na_{0.7}CoO_2$ over the whole temperature range.

For the $x=0.37$ and 0.39 samples, the resistivity is metallic at high temperatures, but exhibits a semiconducting behavior ($d\rho/dT<0$) at low temperatures. The low-T upturn is probably due to the effect of localization as well as the magnetic correlation of Co^{4+} ions. Similar upturns in resistivity were also observed in Na_xCoO_2.[27,32]

The conductivity of $Sr_{0.35}CoO_2$ is the largest among all the Sr_xCoO_2 samples. This could be the result of a large

density of states at Fermi surface as indicated by the large electronic specific-heat coefficient 28.71 $mJ/mol\,K^2$ and a well-defined Sr order in $Sr_{0.35}CoO_2$. The semiconductive behavior of the Sr-poor samples might be related to the carrier localization, which is consistent with the larger localized moment for the Sr-poor samples shown in the magnetic measurements. Systematic structural analysis of $Ca(Sr)_xCoO_2$ $(0.15 \leq x \leq 0.35)$ materials suggests that the $\mathbf{q}_2 = \mathbf{a}^*/2$ modulation changes progressively with a reduction of Ca(Sr) concentration.[18,19] This modulation can strongly influence the band structure and change the behavior of resistivity, especially for the Sr-poor samples.

The metallic to semiconducting crossover in the resistivity of Sr_xCoO_2 with decreasing cation concentration is different than the resistivity behavior of Na_xCoO_2. The resistivity of Na_xCoO_2 is generally metallic with high electrical conductivity except in the charge ordered insulating phase around $x \sim 0.5$. It suggests that the physical properties of Na_xCoO_2 are not generic of the systems with triangular Co lattices.

IV. CONCLUSIONS

In summary, polycrystalline samples of Sr_xCoO_2 $(0.15 \leq x \leq 0.40)$ were prepared by the low-temperature ion exchange technique. Powder XRD analysis shows that these samples are isomorphic to γ-Na_xCoO_2 with a layered hexagonal structure. A systematic study of magnetic and transport properties has been presented. The magnetic susceptibility of all Sr_xCoO_2 samples shows a Curie-Weiss-like temperature dependence above 50 K, but deviates from the Curie-Weiss law and shows a shallow and broad peak at low temperatures under high fields. The effective magnetic moments increase with decreasing strontium content. Large values of electronic specific-heat coefficient γ are obtained for Sr_xCoO_2. The C/T-T^2 curves for Sr_xCoO_2 bend downwards at low temperatures, different than the upturn behavior of the specific heat for Na_xCoO_2. Different transport behaviors were observed for Sr_xCoO_2 with varying x. The resistivity undergoes a semiconducting to metallic crossover with increasing Sr content. In general, Sr_xCoO_2 behaves differently from its precursor Na_xCoO_2.

ACKNOWLEDGMENTS

We would like to thank C. Q. Jin and R. C. Yu for helpful discussions. This work was supported by the National Natural Science Foundation of China and by the Knowledge Innovation Project of Chinese Academy of Sciences.

*Corresponding author. Electronic address: JLLuo@aphy.iphy.ac.cn

[1] M. L. Foo, Y. Wang, S. Watauchi, H. W. Zandbergen, Tao He, R. J. Cava, and N. P. Ong, Phys. Rev. Lett. **92**, 247001 (2004).
[2] K. Takada, H. Sakurai, E. T. Muromachi, F. Izumi, R A. Dilanian, and T. Sasaki, Nature (London) **422**, 53 (2003).
[3] I. Terasaki, Y. Sasago, and K. Uchinokura, Phys. Rev. B **56**, R12685 (1997).
[4] R. E. Schaak, T. Klimczuk, M. L. Foo, and R. J. Cava, Nature (London) **424**, 527 (2003).
[5] Q. Huang, M. L. Foo, J. W. Lynn, W. Zandbergen, G. Lawes, Y. Y. Wang, B. H. Toby, A. P. Ramirez, N. P. Ong, and R. J. Cava, J. Phys.: Condens. Matter **5803**, 16 (2004).
[6] B. C. Sales, R. Jin, K. A. Affholter, P. Khalifah, G. M. Veith, and D. Mandrus, Phys. Rev. B **70**, 174419 (2004).
[7] H. Sakurai, N. Tsujii, and E. Takayama-Muromachi, J. Phys. Soc. Jpn. **73**, 2393 (2004).
[8] J. L. Luo, N. L. Wang, G. T. Liu, D. Wu, X. N. Jing, F. Hu, and T. Xiang, Phys. Rev. Lett. **93**, 187203 (2004).
[9] T. Motohashi, R. Ueda, E. Naujalis, T. Tojo, I. Terasaki, T. Atake, M. Karppinen, and H. Yamauchi, Phys. Rev. B **67**, 064406 (2003).
[10] J. Sugiyama, H. Itahara, J. H. Brewer, E. J. Ansaldo, T. Motohashi, M. Karppinen, and H. Yamauchi, Phys. Rev. B **67**, 214420 (2003).
[11] T. Kawata, Y. Iguchi, T. Itoh, K. Takahata, and I. Terasaki, Phys. Rev. B **60**, 10584 (1999).
[12] Y. Ando, N. Miyamoto, K. Segawa, T. Kawata, and I. Terasaki, Phys. Rev. B **60**, 10580 (1999).
[13] T. Nagira, M. Ito, S. Katsuyama, and H. Nagai, *20th International Conference on Thermoelectrics* (2001).
[14] T. Kajitani, Y. Ono, Y. Miyazaki, and Y. Morii, *21st International Conference on Thermoelectrics* (2002).
[15] B. L. Cushing and J. B. Wiley, J. Solid State Chem. **141**, 385 (1998).
[16] R. Ishikawa, Y. Ono, Y. Miyazaki, and T. Kajitani, Jpn. J. Appl. Phys., Part 2 **41**, L337 (2002).
[17] R. J. Xiao, H. X. Yang, L. F. Xu, H. R. Zhang, Y. G. Shi, and J. Q. Li, Solid State Commun. **135**, 687 (2005).
[18] H. X. Yang, Y. G. Shi, Y. Q. Guo, X. Liu, R. J. Xiao, J. L. Luo, and J. Q. Li, cond-mat/0503136 (unpublished).
[19] H. X. Yang, Y. G. Shi, X. Liu, R. J. Xiao, H. F. Tian, and J. Q. Li, Phys. Rev. B **73**, 014109 (2006).
[20] Kazunori Takada, Katsutoshi Fukuda, Minoru Osada, Izumi Nakai, Fujio Izumi, Ruben A. Dilanian, Kenichi Kato, Masaki Takata, Hiroya Sakurai, Eiji Takayama-Muromachid, and Takayoshi Sasakia, J. Mater. Chem. **14**, 1448 (2004).
[21] M. L. Foo, R. E. Schaak, V. L. Miller, T. Klimczuk, N. S. Rogado, Y. Wang, G. C. Lau, C. Craley, H. W. Zandbergen, N. P. Ong, and R. J. Cava, Solid State Commun. **127**, 33 (2003).
[22] G. G. Amatucci, J. M. Tarascon, and L. C. Klein, J. Electrochem. Soc. **143**, 1114 (1996).
[23] H. X. Yang, Y. Xia, Y. G. Shi, H. F. Tian, R. J. Xiao, X. Liu, Y. L. Liu, and J. Q. Li, Phys. Rev. B **74**, 094301 (2006).
[24] R. Ray, A. Ghoshray, K. Ghoshray, and S. Nakamura, Phys. Rev. B **59**, 9454 (1999).
[25] D. J. Singh, Phys. Rev. B **68**, 020503(R) (2003).
[26] A. T. Boothroyd, R. Coldea, D. A. Tennant, D. Prabhakaran, L. M. Helme, and C. D. Frost, Phys. Rev. Lett. **92**, 197201 (2004).
[27] S. P. Bayrakci, C. Bernhard, D. P. Chen, B. Keimer, R. K. Kremer, P. Lemmens, C. T. Lin, C. Niedermayer, and J. Strempfer,

Phys. Rev. B **69**, 100410(R) (2004).
[28] S. P. Bayrakci, I. Mirebeau, P. Bourges, Y. Sidis, M. Enderle, J. Mesot, D. P. Chen, C. T. Lin, and B. Keimer, Phys. Rev. Lett. **94**, 157205 (2005).
[29] L. M. Helme, A. T. Boothroyd, R. Coldea, D. Prabhakaran, D. A. Tennant, A. Hiess, and J. Kulda, Phys. Rev. Lett. **94**, 157206 (2005).
[30] M. Bhwiler, B. Batlogg, S. M. Kazakov, and J. Karpinski, cond-mat/0309311 (unpublished).
[31] R. Jin, B. C. Sales, S. Li, and D. Mandrus, Phys. Rev. B **72**, 060512(R) (2005).
[32] M. Mikami, M. Yoshimura, Y. Mori, T. Sasaki, R. Funahashi, and M. Shikano, Jpn. J. Appl. Phys., Part 1 **42**, 7383 (2003).